Earth's water may have been inherited from material similar to enstatite chondrite meteorites

Laurette Piani[1*], Yves Marrocchi[1], Thomas Rigaudier[1], Lionel G. Vacher[1,2], Dorian Thomassin[1], Bernard Marty[1]

[1]Centre de Recherches Pétrographiques et Géochimiques (CRPG), Centre National de Recherche Scientifique (CNRS)-Université de Lorraine, Vandoeuvre-les-Nancy, F-54500, France

[2]Department of Physics, Washington University in St. Louis, St. Louis, MO, USA

*Correspondence to: laurette.piani@univ-lorraine.fr

Abstract (132/125 words):

The origin of Earth's water remains unknown. Enstatite chondrite (EC) meteorites have similar isotopic composition to terrestrial rocks, so are often considered representative of the material which formed Earth. ECs are presumed to be devoid of water because they formed in the inner Solar System. Earth's water is thus generally attributed to a late addition of a small fraction of hydrated materials, such as carbonaceous chondrite meteorites, which originated in the outer Solar System where water was more abundant. We show that EC meteorites contain sufficient hydrogen to have delivered to Earth at least three times the mass of water in its oceans. Because EC hydrogen and nitrogen isotopic compositions match those of Earth's mantle, EC-like asteroids might have been major contributors of these volatile elements to the Earth's crust and mantle.

Main text (2756 words):

The origin of Earth's water is debated. The isotopic composition of Earth suggests that it is composed of material from the inner Solar System, such as enstatite chondrite (EC) meteorites (*1-3*). The inner Solar System was too warm to have retained water ice, so terrestrial water is thought to have been supplied by hydrated materials that originally formed in the outer Solar System before migrating inwards (*4, 5*).

Hydrogen isotopic compositions are conventionally expressed as $\delta D \equiv [(D/H)_{sample}/(D/H)_{SMOW} - 1] \times 1000$, where D/H is the ratio of ^2H (deuterium) to ^1H (protium), and standard mean ocean water (SMOW) is the mean value of Earth's oceans. δD varies greatly among Solar System objects. The bulk protosolar nebula had δD = –865‰, estimated from the solar wind and remnant H_2 in the atmospheres of the giant planets (*6*). Compared to this protosolar value, all other materials in the Solar System are enriched in deuterium, with inner Solar System objects having intermediate values e.g., δD ≡ 0‰ in terrestrial oceans and –165 to +800‰ in asteroids, as recorded in primitive meteorites (*7*). Outer Solar System objects, such as comets, are even more enriched in deuterium, up to δD = 2,400‰ in comet 67P/Churyumov-Gerasimenko (*8*). Among meteorites, water-rich carbonaceous chondrites of Ivuna-type (CI) and Mighei-type (CM) are potential sources of terrestrial water because their δD values are distributed around a value coincident with Earth's oceans e.g., δD ≡ 0‰ (*9*). Dynamical simulations suggest that the so-called C-type (carbonaceous) asteroids −whose optical properties suggest a genetic link to water-rich carbonaceous chondrites− could have been scattered into the inner solar system from beyond

the orbit of Jupiter [e.g., (*10*)], potentially delivering water to Earth during or after its main phase of accretion throughout the first millions of years of the Solar System formation.

An alternative possibility is that EC-like materials, which have similar isotopic abundances to Earth for some key elements like oxygen, titanium, calcium, molybdenum (*3*), could contain enough hydrogen with the appropriate isotopic composition to provide water to the growing proto-Earth. Testing this scenario has been hampered by difficulties in measuring H concentrations and isotopic ratios in ECs, due to their assumed low H abundances and the potential for terrestrial contamination (*7*).

We measured H abundances and isotopic compositions for a suite of thirteen ECs that spans the full range of thermal metamorphism degrees (i.e., represented by the petrologic types 3 for the least metamorphosed to 6 for the chondrites the most altered by thermal metamorphism on the parent asteroid) to evaluate potential effects of parent body processing that could have altered the original water content and H isotopic composition (*11*). We also analyzed one aubrite meteorite (Norton County), which represents an evolved planetary body of enstatite meteorite composition for which metal-silicate segregation (differentiation) occurred (*11*). Hydrogen measurements were performed at the Centre de Recherches Pétrographiques et Géochimiques (CRPG, Nancy, France), either on bulk samples with an elemental analyzer (EA) coupled to a stable isotope ratio mass spectrometer (IRMS), or at the micron scale using a secondary ion mass spectrometer (SIMS) (*11*).

We find the enstatite chondrites have bulk hydrogen contents (reported as water equivalents) ranging from 0.08 to 0.54 wt.% H_2O (Fig. 1A, Table S2). The EH3 meteorites are generally more H rich (0.44 ± 0.04 wt.% H_2O, all uncertainties are one standard deviation unless otherwise noted) than the more metamorphosed groups EH4 (0.2 ± 0.1 wt.% H_2O), EH5 (0.3 ± 0.1 wt.% H_2O), and EL6 (0.3 ± 0.3 wt.% H_2O). The Norton County aubrite is 0.3 ± 0.2 wt.% H_2O. These EC water contents are well below those measured in the water-rich carbonaceous chondrites Orgueil (CI), Alais (CI), and Murchison (CM), which are 7.2–9.1 wt.% H_2O (Fig. 1A, Table S2). However, all analyzed ECs contain hydrogen concentrations above the EA-IRMS detection limit (~0.05 wt.% H_2O; (*11*)). The least-altered EH chondrites (EH3 and EH4) show δD values systematically below the current value of Earth's oceans (averaging δD = –103 ± 3‰), whereas metamorphosed ECs (EH5 and EL6) and the aubrite have even lower values, averaging δD = –127 ± 15‰ (Fig. 1B, Table S2).

If the hydrogen contents had been totally due to atmospheric contamination during sample preparation, constant D/H ratios would be observed despite variable H concentrations. Instead, our data follow a negative trend in a δD *vs.* 1/H diagram (Fig. S5), indicating possible loss of D-enriched hydrogen-bearing organic molecules (*12*) during thermal metamorphism within the EC parent asteroid(s). In the least metamorphosed sample we analyzed, the pristine EH3 meteorite Sahara 97096 [EH3.1–3.4 (*13*); fragment of the same meteorite as Sahara 97116 in Table S2], only a thin (≈500 μm) surface layer of terrestrial alteration is visible (*11*); its inner portions remain unaffected, as attested by the presence of unaltered oldhamite (CaS) grains, a highly hydrophilic mineral (*14, 15*). The fresh interior of Sahara 97096 has lower (and constant) H contents (0.5 ± 0.1 wt.% H_2O) than the altered parts (3.0 ± 1.1 wt.% H_2O), and their H isotopic compositions are also different (fresh interior δD = –103.6 ± 0.7‰, altered surface δD = –136.3 ± 3.9‰; Fig. S4, Table S2). Similar features have been observed in Martian meteorites subjected to desert alteration, with the H content and isotopic characteristics being modified only at the near surface (i.e., <2 mm) (*16*). In addition, the hydrogen contents and D/H ratios measured for the two meteorite finds (Sahara 97096 and Yamato 791790) are very close to the ones measured for the Indarch chondrite that has collected after its observed fall and consistent with a metamorphic evolution of the H signatures in ECs (Table S2; Fig. S5B). These observations suggest that the H contents of

ECs were established during the early Solar System and have experienced minimal modifications on Earth.

To confirm the indigenous nature of H in the interiors of ECs, we used SIMS to analyze the H contents and isotopic compositions of the glass fraction (mesostasis) in four chondrules -sub-millimetre silicate spherules that correspond to the main mineral assemblages in ECs- of Sahara 97096, the least-metamorphosed EC in our sample (*11, 12*). For comparison, we performed similar measurements in two CV chondrites (Kaba and Vigarano) having the same degree of metamorphism (*17*). The glassy mesostasis of Sahara 97096 contains between 2,700 and 12,300 wt. ppm H_2O equivalent, with an average value of 7,560 ± 1,546 wt. ppm H_2O (two standard deviations, 2σ) for 16 measurements (Fig. 1C, Table S4). Although their metamorphic grades are similar to Sahara 97096, the CV chondrites Vigarano and Kaba show lower H contents of 330 ± 140 and 210 ± 120 wt. ppm H_2O, respectively (Fig. 1C, Table S4). The H isotopic composition of Sahara 97096 mesostasis is homogeneous with an average δD value of –147 ± 16‰ (2σ; Fig. 1D, Table S4), whereas Vigarano and Kaba show δD = –261 ± 25 and +17 ± 95‰, respectively (2σ; Fig. 1D, Table S4). Among these three meteorites, only Kaba underwent aqueous alteration of its chondrules (*18*), which accounts for the variable D/H ratio of its mesostasis. Vigarano contains traces of incipient aqueous alteration restricted to its fine-grained matrix (*19*). As Sahara 97096 does not show any evidence of aqueous alteration, the abundant H contents of its chondrule mesostases was thus acquired before the EC parent asteroid evolution, possibly when chondrule formed.

Considering the H concentration of Sahara 97096 mesostasis, the modal abundance of mesostasis in Sahara 97096 chondrules [16.2 vol.% (*15*)] and the modal abundance of chondrules in ECs [~70 vol.% (*20*)], H in chondrule mesostases accounts for 702 ± 117 wt. ppm H_2O of the bulk rock, or ~13% of the bulk-rock H content. Another potential source of H in ECs is insoluble organic matter (IOM). However, given the low abundance of IOM in ECs (0.6 wt.%) and the H concentration in EC organics [0.7 wt.% (*12*)], the contribution of IOM to the bulk-rock H content is only 380 ppm H_2O, or 7.7% of the total H content of the chondrite. Combined, H hosted in chondrule mesostases and IOM can only account for ~20% of the total H measured in the Sahara 97096 bulk rock.

H concentrations have been reported in low-calcium pyroxenes from non-carbonaceous chondrite materials from (i) the S-type asteroid Itokawa (700–1,000 wt. ppm H_2O) brought back by the Hayabusa sample-return spacecraft and (ii) the metamorphosed ordinary chondrite Larkman Nunatak 12036 (600–1,300 wt. ppm H_2O) (*21*). We found an even higher H concentration (5,300 wt. ppm H_2O; Table S2) for the pyroxene fraction of the Norton County aubrite. The modal abundance of low-calcium pyroxene in ECs is ~50 vol.% (*15*), so enstatite pyroxenes could account for ~15% or ~58% of the bulk H content of ECs considering the highest H-content of OC pyroxenes (1,300 wt. ppm H_2O) or the aubrite pyroxene fraction, respectively. The remaining ~65% to 20% of H measured in the bulk rock may be contributed by other unknown carriers such as sulfur-rich carbon-bearing porous amorphous silica (*22*), due to an underestimation of the H content in EC pyroxenes, and/or could derive from some pervasive terrestrial contamination, although a limited amount of contamination is expected otherwise it would have erased the thermal metamorphism effect visible on the δD *vs.* 1/H diagram (Fig. S5). Our SIMS measurements demonstrate that at least 20% of the H in ECs has an identified carrier phase (mesostasis or IOM) and that most of the remaining 80% is probably of indigenous origin. This implies that terrestrial hydrogen could be derived from ECs without invoking additional sources.

We incorporated the H concentrations measured in ECs (Tables S2 and S4) into theoretical models of Earth's formation that invoke mixing of chondrite-like materials. These models utilize various proportions of enstatite, ordinary, and carbonaceous chondrite-like materials,

e.g. (*1-3*, *5, 23*), so we explored three end-member compositions: (i) 100% EC-like materials (*1*), (ii) 68% EC-like and 32% carbonaceous chondrite-like materials (*2, 23*), although these proportions could be inconsistent for the isotopic composition of the Earth's mantle *(11)*, and (iii) ~70% EC-like, ~25% ordinary chondrite-like, and ~5% carbonaceous chondrite-like materials (*3*) (Fig. 2). In all cases, EC-like materials contribute substantially to Earth's water budget, supplying 3.4 to 23.1 times the mass of Earth's oceans (1.4×10^{21} kg) once our H content measurements are included (Table S2). These estimates are upper limits because loss of volatiles might have occurred during Earth's accretion e.g. (*24, 25*). Considering only identified H-bearing phases (mesostasis and IOM), EC-like materials alone contribute ~3 to 4.5 times the mass of Earth's oceans (Fig. 2). If Sahara 97096 is representative of the most pristine ECs (Fig. 2), its bulk-rock hydrogen content (4,700 wt. ppm H_2O or ≥14 ocean masses) is sufficient to explain the highest estimates of the water content of Earth's surface and mantle, which are 1,000–3,900 ppm H_2O (*5, 26*). Mesostasis and IOM H contents alone can account for 3 to 5 times the total mass of the oceans, corresponding to intermediate estimates of Earth's mantle water content.

The hydrogen isotopic composition of ECs is depleted in deuterium relative to Earth's oceans, but within the range of mantle values (Fig. 3). ECs are not the only group of meteorites with D-poor values consistent with Earth's mantle, as CM-type carbonaceous chondrites also span the range of mantle H isotopic compositions (Fig. 3). Nitrogen isotopes provide additional constraints (*27*), as the mantle is depleted in both D and ^{15}N relative to the surface reservoirs (atmosphere and oceans). Combining H and N isotopic compositions allows us to identify potential chondritic precursors (Fig. 4). Only ECs are compatible with both the δD and $\delta^{15}N$ values measured in mantle-derived rocks (Fig. 4). D-poor solar hydrogen (δD = –865‰; (*6*)) could also have contributed to the mantle composition (*28*), although it would require extreme enrichments of solar H relative to solar Ne because mantle neon is solar-like. The chondritic H/Ne ratio [4×10^8 (*29*)] is five orders of magnitude higher than the solar ratio [7.9×10^3 (*30*)]. Therefore we favor the incorporation of EC-like material in the silicate Earth (*1*).

Earth's surficial (oceans and atmosphere) H and N isotopic compositions (δD ≡0‰ and $\delta^{15}N \equiv 0$‰) cannot be easily derived from EC materials alone because they are more rich in D by ~100–200‰ and ^{15}N by 5–40‰. Atmospheric escape to space, often invoked for atmospheric species including water vapor, could potentially achieve such enrichments, but light noble gases do not support this hypothesis. Ne-Ar isotopic variations in the mantle-atmosphere system do not follow elemental/isotopic variations that would sign atmospheric escape; they are best reproduced by mixing between a solar-like component trapped in the solid Earth and a carbonaceous chondrite-like component with a low $^{20}Ne/^{22}Ne$ ratio (*5*). A contribution of carbonaceous chondrite-like materials, especially CIs, to the surface inventory would also be consistent with the observed H and N isotopic variations (Fig. 4) and can be computed independently from H and N isotopic ratios (*11*). We find a ~4% contribution from CI-like material to the Earth surficial reservoir based on hydrogen abundances and isotopic compositions, and a ~15% contribution based on equivalent data for nitrogen (*11*). Although nitrogen isotopes could also have contributions from cometary materials (*11*), these estimates are similar to those obtained from noble gases (*5*) and molybdenum isotopes (*23*). We cannot determine exactly when the CI-like material was delivered to the surficial reservoir, but we note that it must have been sufficiently late during Earth's formation to prevent a global re-homogenization of the mantle with the surface.

Acknowledgments:
We thank the Field Museum (Chicago, USA), the French National Museum of Natural History (Paris, France), the Japanese National Institute for Polar Research (Tokyo, Japan), the

University of New Mexico (Albuquerque, USA), Natural History Museum (Vienna, Austria) and the CEREGE meteoritic collection (Aix en Provence, France) for providing the meteorites samples. We thank Nordine Bouden and the members of the Ion Probe Team Nancy (IPTN) for help with the SIMS. We thank E. Deloule, A. Gurenko, L. France, M. Broadley, D. Bekaert, and C. Cartier for fruitful discussions. This is CRPG contribution #2997. **Funding:** Supported by the French Research National Agency (grant No. ANR-19-CE31-0027-01 to L.P.) and by the European Research Council (grant No. 695618 to B.M.). **Author contributions:** L.P. designed the study; L.P., T.G., L.G.V., and D.T. performed the bulk and *in-situ* analyses. Y.M. and B.M. contributed to the experimental design. L.P., Y.M., and B.M. discussed the data and wrote the manuscript. All authors provided input to the data analysis and manuscript preparation. **Competing interests:** We declare no competing interests. **Data and materials availability:** All meteorites we studied are deposited in public museums, as listed in the supplementary material. Our measured H abundances and D/H ratios, for the meteorite samples and standards, are listed in Tables S1-S4 and Data S1.

Supplementary materials:

Materials and Methods
Tables S1–S6
Figs. S1–S6
Data S1
References (*36–62*)

References

1. M. Javoy *et al.*, The chemical composition of the Earth: Enstatite chondrite models. *Earth Planet. Sci. Lett.* **293**, 259–268 (2010).
2. P. H. Warren, Stable-isotopic anomalies and the accretionary assemblage of the Earth and Mars: A subordinate role for carbonaceous chondrites. *Earth Planet. Sci. Lett.* **311**, 93–100 (2011).
3. N. Dauphas, The isotopic nature of the Earth's accreting material through time. *Nature*. **541**, 521–524 (2017).
4. A. Morbidelli *et al.*, Source regions and timescales for the delivery of water to the Earth. *Meteoritics* **35**, 1309–1320 (2000).
5. B. Marty, The origins and concentrations of water, carbon, nitrogen and noble gases on Earth. *Earth Planet. Sci. Lett.* **313–314**, 56–66 (2012).
6. G. Gloeckler, J. Geiss, in *Primordial Nuclei and Their Galactic Evolution*, N. Prantzos, M. Tosi, R. Von Steiger, Eds. (Springer Netherlands, Dordrecht, 1998), pp. 275–284.
7. C. M. O'D. Alexander *et al.,* The Provenances of Asteroids, and Their Contributions to the Volatile Inventories of the Terrestrial Planets. *Science* **337**, 721–723 (2012).
8. K. Altwegg *et al.*, Time variability and heterogeneity in the coma of 67P/Churyumov-Gerasimenko. *Science* **347**, 2–5 (2015).
9. F. Robert, The D/H Ratio in Chondrites. *Space Sci. Rev.* **106**, 87 (2003).
10. S. N. Raymond, A. Izidoro, Origin of water in the inner Solar System: Planetesimals scattered inward during Jupiter and Saturn's rapid gas accretion. *Icarus* **297**, 134–148 (2017).
11. Materials and methods are available as supplementary materials.
12. L. Piani *et al.*, Structure, composition, and location of organic matter in the enstatite chondrite Sahara 97096 (EH3). *Meteoritics* **47**, 8–29 (2012).
13. E. Quirico, M. Bourot-denise, C. Robin, G. Montagnac, P. Beck, A reappraisal of the metamorphic history of EH3 and EL3 enstatite chondrites. *Geochim. Cosmochim. Acta* **75**, 3088–3102 (2011).

14. M. K. Weisberg, M. Prinz, Sahara 97096: A highly primitive EH3 chondrite with layered sulfide-metal-rich chondrules. *Mar. Chem.*, 1741 (1998).
15. L. Piani, Y. Marrocchi, G. Libourel, L. Tissandier, Magmatic sulfides in the porphyritic chondrules of EH enstatite chondrites. *Geochim. Cosmochim. Acta* **195**, 84–99 (2016).
16. A. Stephant, L. A. J. Garvie, P. Mane, R. Hervig, M. Wadhwa, Terrestrial exposure of a fresh Martian meteorite causes rapid changes in hydrogen isotopes and water concentrations. *Sci. Rep.* **8**, 6–12 (2018).
17. L. Bonal, E. Quirico, M. Bourot-Denise, G. Montagnac, Determination of the petrologic type of CV3 chondrites by Raman spectroscopy of included organic matter. *Geochim. Cosmochim. Acta* **70**, 1849–1863 (2006).
18. L. P. Keller, P. R. Buseck, Aqueous alteration in the Kaba CV3 carbonaceous chondrite. *Geochim. Cosmochim. Acta* **54**, 2113–2120 (1990).
19. M. R. Lee, R. Hutchison, A. L. Graham, Aqueous alteration in the matrix of the Vigarano (CV3) carbonaceous chondrite. *Meteorit. Planet. Sci.* **31**, 477–483 (1996).
20. E. R. D. Scott, A. N. Krot, in *Meteorites and Cosmochemical Processes, Volume 1 of Treatise on Geochemistry (Second Edition). Elsevier. Edited by Andrew M. Davis*, pp. 65–137 (2014).
21. Z. Jin, M. Bose, New clues to ancient water on Itokawa. *Sci. Adv.* **5**, 1–10 (2019).
22. S. W. Lehner, P. Németh, M. I. Petaev, P. R. Buseck, Porous, S-bearing silica in metal-sulfide nodules and in the interchondrule clastic matrix in two EH3 chondrites. *Meteoritics* **52**, 2424–2436 (2017).
23. G. Budde, C. Burkhardt, T. Kleine, Molybdenum isotopic evidence for the late accretion of outer Solar System material to Earth. *Nat. Astron. 3*, 1–6 (2019).
24. K. Hamano, Y. Abe, H. Genda, Emergence of two types of terrestrial planet on solidification of magma ocean. *Nature* **497**, 607–610 (2013).
25. H. Lammer *et al.*, Origin and loss of nebula-captured hydrogen envelopes from 'sub'- to "super-Earths" in the habitable zone of Sun-like stars. *Mon. Not. R. Astron. Soc.* **439**, 3225–3238 (2014).
26. A. H. Peslier, M. Schönbächler, H. Busemann, S. I. Karato, Water in the Earth's Interior: Distribution and Origin. *Space Sci. Rev.* **212**, 1–68 (2017).
27. M. Javoy, F. Pineau, D. Demaiffe, Nitrogen and carbon isotopic composition in the diamonds of Mbuji Mayi (Zaïre). *Earth Planet. Sci. Lett.* **68**, 399–412 (1984).
28. L. J. Hallis *et al.*, Evidence for primordial water in Earth's deep mantle. *Science* **350**, 795–797 (2015).
29. B. Marty *et al.*, Origins of volatile elements (H, C, N, noble gases) on Earth and Mars in light of recent results from the ROSETTA cometary mission. *Earth Planet. Sci. Lett.* **441**, 91–102 (2016).
30. K. Lodders, Solar System Abundances and Condensation Temperatures of the Elements. *Astrophys. J.* **591**, 1220–1247 (2003).
31. L. Piani, F. Robert, L. Remusat, Micron-scale D/H heterogeneity in chondrite matrices: A signature of the pristine solar system water? *Earth Planet. Sci. Lett.* **415**, 154–164 (2015).
32. E. Deloule, F. Albarède, S. M. F. Sheppard, Hydrogen isotope heterogeneities in the mantle from ion probe analysis of amphiboles from ultramafic rocks. *Earth Planet. Sci. Lett.* **105**, 543–553 (1991).
33. M. W. Loewen, D. W. Graham, I. N. Bindeman, J. E. Lupton, M. O. Garcia, Hydrogen isotopes in high $^{3}He/^{4}He$ submarine basalts: Primordial vs. recycled water and the veil of mantle enrichment. *Earth Planet. Sci. Lett.* **508**, 62–73 (2019).
34. M. M. Grady, I. P. Wright, L. P. Carr, C. T. Pillinger, Compositional differences in

enstatite chondrites based on carbon and nitrogen stable isotope measurements. *Geochim. Cosmochim. Acta* **50**, 2799–2813 (1986).
35. P. Cartigny, B. Marty, Nitrogen isotopes and mantle geodynamics: The emergence of life and the atmosphere-crust-mantle connection. *Elements* **9**, 359–366 (2013).

References in Supplementary Materials

36. G. T. Prior, The meteorites of Uwet, Kota Kota and Angela: re-determinations of nickel and iron in the Baroti and Wittekranz meteoric stones. *Mineral. Mag.* **17**, 127–134 (1914).
37. M. M. M. Meier, C. Cloquet, B. Marty, Mercury (Hg) in meteorites: Variations in abundance, thermal release profile, mass-dependent and mass-independent isotopic fractionation. *Geochim. Cosmochim. Acta* **182**, 55–72 (2016).
38. M. Lupker *et al.*, Predominant floodplain over mountain weathering of Himalayan sediments (Ganga basin). *Geochim. Cosmochim. Acta* **84**, 410–432 (2012).
39. A. Ando, New silicate the rock reference Survey materials of Japan , issued from Geological. *Geochem. J.* **18**, 215–216 (1984).
40. URL of the IAEA database: https://nucleus.iaea.org/sites/ReferenceMaterials/Pages/Stable-Isotopes.aspx
41. M. C. Liu, K. D. McKeegan, T. M. Harrison, G. Jarzebinski, L. Vltava, The Hyperion-II radio-frequency oxygen ion source on the UCLA ims1290 ion microprobe: Beam characterization and applications in geochemistry and cosmochemistry. *Int. J. Mass Spectrom.* **424**, 1–9 (2018).
42. T. H. Druitt *et al.*, Magma Storage and Extraction Associated with Plinian and Interplinian Activity at Santorini Caldera (Greece). *J. Petrol.* **57**, 461–494 (2016).
43. C. Aubaud *et al.*, Intercalibration of FTIR and SIMS for hydrogen measurements in glasses and nominally anhydrous minerals. *Am. Mineral.* **92**, 811–828 (2007).
44. G. Mollex, Architecture de la plomberie du volcan carbonatitique Oldoinyo Lengai : nouvelles contraintes sur la source, les transferts hydrothermaux, et la différenciation magmatique dans la chambre active, PhD thesis, Lorraine University, France (2017).
45. B. Marty *et al.*, Xenon isotopes in 67P/Churyumov-Gerasimenko show that comets contributed to Earth's atmosphere. *Science* **356**, 1069–1072 (2017).
46. D. Bockelée-Morvan *et al.*, Cometary Isotopic Measurements. *Space Sci. Rev.* **197**, 47–83 (2015).
47. P. Ardia, M. M. Hirschmann, A. C. Withers, B. D. Stanley, Solubility of CH4 in a synthetic basaltic melt, with applications to atmosphere-magma ocean-core partitioning of volatiles and to the evolution of the Martian atmosphere. *Geochim. Cosmochim. Acta* **114**, 52–71 (2013).
48. M. M. Hirschmann, A. C. Withers, P. Ardia, N. T. Foley, Solubility of molecular hydrogen in silicate melts and consequences for volatile evolution of terrestrial planets. *Earth Planet. Sci. Lett.* **345–348**, 38–48 (2012).
49. C. Cartier, B. J. Wood, The role of reducing conditions in building mercury. *Elements* **15**, 39–45 (2019).
50. V. Clesi *et al.*, Low hydrogen contents in the cores of terrestrial planets. *Sci. Adv.* **4**, 3, e1701876 (2018)
51. A. E. Rubin, Impact features of enstatite-rich meteorites. *Chem. Erde-Geochem.* **75**, 1–28 (2015).
52. R. Yokochi, B. Marty, A determination of the neon isotopic composition of the deep

mantle. *Earth Planet. Sci. Lett.* **225**, 77–88 (2004).
53. C. D. Williams, S. Mukhopadhyay, Capture of nebular gases during Earth's accretion is preserved in deep-mantle neon. *Nature* **565**, 78–81 (2019).
54. H. Genda, Y. Abe, Enhanced atmospheric loss on protoplanets at the giant impact phase in the presence of oceans. *Nature* **433**, 842–844 (2005).
55. M. Fischer-Gödde, T. Kleine, Ruthenium isotopic evidence for an inner Solar System origin of the late veneer. Nature 541, 525–527 (2017).
56. K. J. Walsh, A. Morbidelli, S. N. Raymond, D. P. O'Brien, A. M. Mandell, A low mass for Mars from Jupiter's early gas-driven migration. *Nature* **475**, 206–209 (2011).
57. F. M. McCubbin, J. J. Barnes, Origin and abundances of H_2O in the terrestrial planets, Moon, and asteroids. *Earth Planet. Sci. Lett.* **526**, 115771 (2019).
58. T. Kleine *et al.*, Hf-W chronology of the accretion and early evolution of asteroids and terrestrial planets. *Geochim. Cosmochim. Acta* **73**, 5150–5188 (2009).
59. I. N. Bindeman, V. S. Kamenetsky, J. Palandri, T. Vennemann, Hydrogen and oxygen isotope behaviors during variable degrees of upper mantle melting: Example from the basaltic glasses from Macquarie Island. *Chem. Geol.* **310–311**, 126–136 (2012).
60. K. P. Jochum *et al.*, MPI-DING reference glasses for in situ microanalysis: New reference values for element concentrations and isotope ratios. *Geochemistry, Geophys. Geosystems*. **7** (2006), doi:10.1029/2005GC001060.
61. E. Hauri *et al.*, SIMS analysis of volatiles in silicate glasses. *Chem. Geol.* **183**, 99–114 (2002).
62. J. Yang, S. Epstein, Interstellar organic matter in meteorites. *Geochim. Cosmochim. Acta* **47**, 2199–2216 (1983).
63. E. Jarosewich, Chemical Analyses of Meteorites: A Compilation of Stony and Iron Meteorite Analyses. *Meteoritics* **25**, 323 (1990).

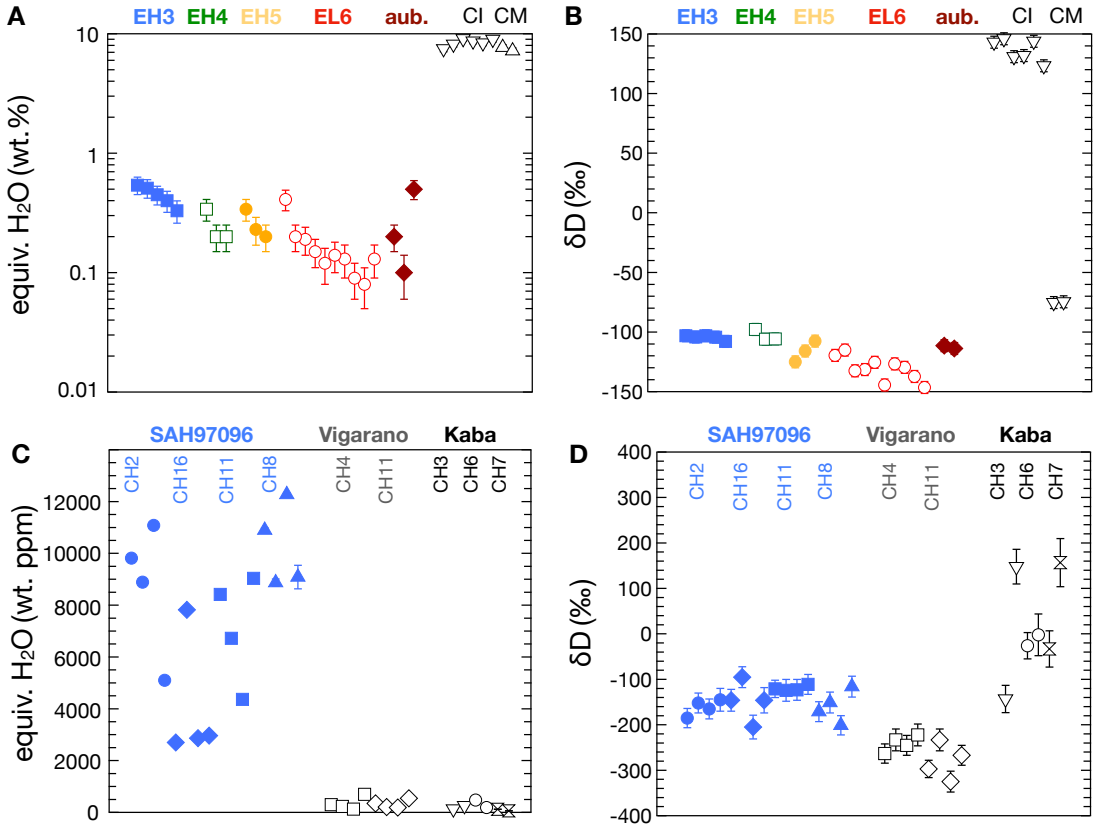

Fig. 1. Hydrogen contents and isotopic compositions of enstatite chondrites. (A) Bulk-rock hydrogen content, reported as water equivalent by weight on a logarithmic scale. (B) Bulk rock deuterium abundance, expressed as an offset from mean ocean water. (C) Mesostasis hydrogen content. (D) Mesostasis deuterium abundance. The CM- and CI-type carbonaceous chondrites Orgueil, Alais, and Murchison, and the aubrite Norton County, are included in panels A and B for comparison. Panels C and D show data for the primitive EC Sahara 97096 (SAH97096; EH3.1–3.4), and the two CV-type carbonaceous chondrites Vigarano and Kaba for comparison *(11)*. Different symbols in panels C and D indicate different chondrules (labeled CH). Error bars are 2σ and are smaller than the symbol size in panel B. The data are listed in Tables S2 and S4.

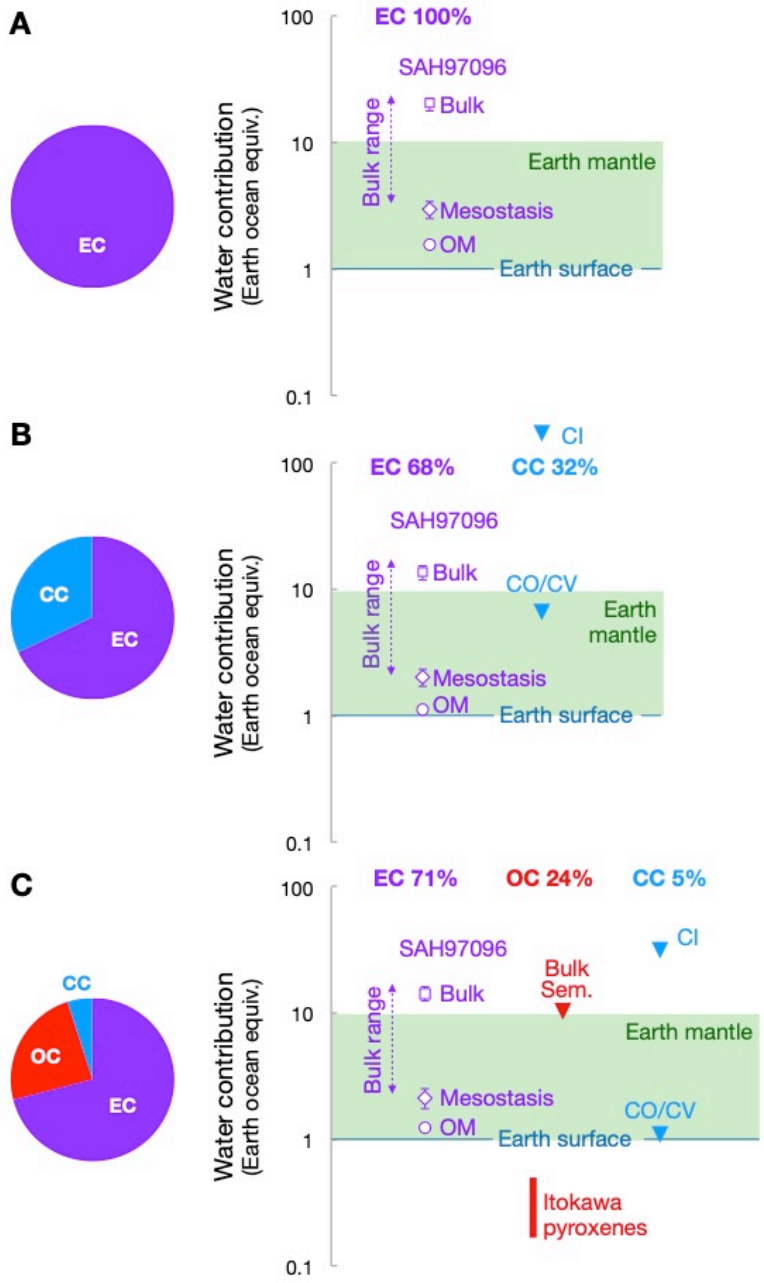

Figure 2. Contributions of accreting materials to Earth's hydrogen budget in three different models. Values are expressed in equivalent ocean masses, where one ocean = 1.4 × 10^{21} kg H_2O. (A) A model Earth comprising only enstatite chondrites (*1*). (B) A model Earth comprising 68% ECs and 32% carbonaceous chondrites (CCs) *(2)*. (C) A model Earth comprising 71% ECs, 24% ordinary chondrites (OCs), and 5% CCs [(*3*), their most extreme case]. The consistency of such models for the isotopic composition of the mantle is discussed in *(11)*. SAH97096 = Sahara 97096 (EH3); Bulk = bulk rock; OM = organic matter; Sem. = Semarkona (LL3.0). Carbonaceous chondrites are divided into water-rich (CI-type) and water-poor groups (CV- and CO-type). Water contribution by ECs are in purple, by OCs are in red, and by CCs in blue. The water content of Earth's mantle (green band) is between 1 and ≥10 ocean masses (*26*). We consider 10 ocean masses in the mantle as a maximum value (green band). Regardless of the model considered, the water provided by ECs alone lies above the maximum value of 10 oceans and thus substantially contributes to the Earth's water budget. Data are from (*5, 7, 11, 21*) and this study (Tables S2 and S4). Error bars are 2σ.

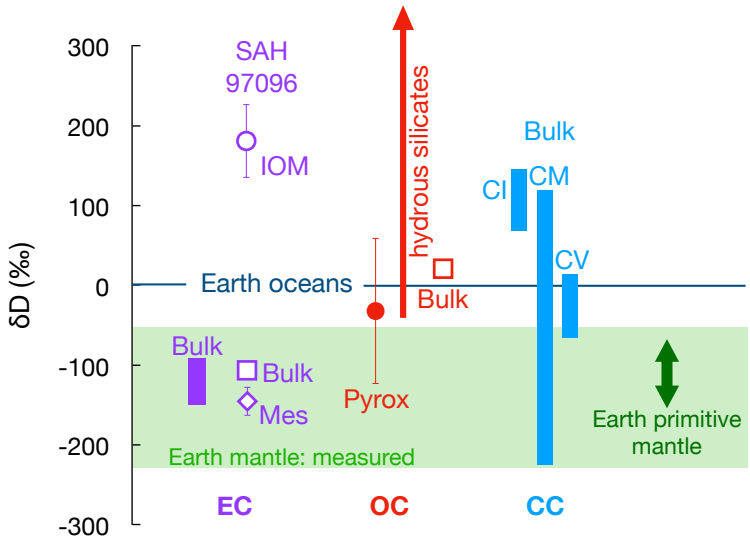

Figure 3. Hydrogen isotopic compositions of meteorites compared to Earth's mantle and oceans. Data are shown for enstatite chondrites (ECs, bulk rock and mesostasis; in purple), ordinary chondrite (OC) pyroxenes and hydrous minerals (in red), and carbonaceous chondrites (CCs, bulk rock, CI-, CM-, and CV-type; in blue). SAH97096 = Sahara 97096 (EH3); Bulk = bulk rock; OM = organic matter; Mes = mesostasis; Pyrox = pyroxene. Meteorite data are from (*7, 12, 21, 31*) and this study (Tables S2 and S4). Values for Earth's mantle (δD = –220 to –20‰, green shaded area) are from (*26*), with the most D-depleted values reported in (*28*). The primitive mantle ranges from δD = –130 to –75‰ (*32*, *33*).

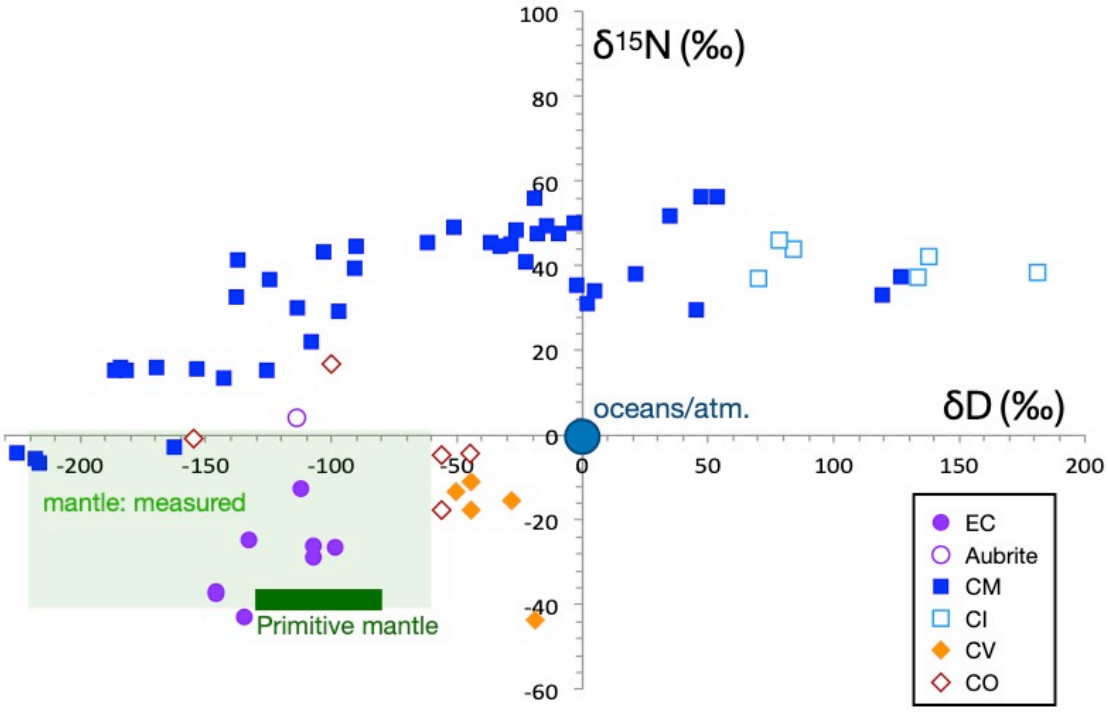

Figure 4. Hydrogen and nitrogen isotopic compositions of meteorites compared to Earth's mantle and surface. Meteorite bulk-rocks values are shown for enstatite chondrites (ECs) and CM-, CI-, CV-, and CO-type carbonaceous chondrites; data are from Table S2 and (*7, 34, 35*). Mantle δD values are from (*26, 28*). The primitive mantle δD is from (*32*) and (*33*) and $\delta^{15}N$ by the most negative values (–40‰) in (*35*).